



Published in final edited form as:

J Biomech. 2020 January 02; 98: 109464. doi:10.1016/j.jbiomech.2019.109464.

The association between periacetabular osteotomy reorientation and hip joint reaction forces in two subgroups of acetabular dysplasia

Brecca M.M. Gaffney^a, John C. Clohisy^b, Linda R. Van Dillen^{a,b}, Michael D. Harris^{a,b,c,*}

^aProgram in Physical Therapy, Washington University in St. Louis School of Medicine, St. Louis, MO, United States

^bDepartment of Orthopaedic Surgery, Washington University in St. Louis School of Medicine, St. Louis, MO, United States

^cDepartment of Mechanical Engineering and Materials Science, Washington University in St. Louis, St. Louis, MO, United States

Abstract

Acetabular dysplasia is primarily characterized by an altered acetabular geometry that results in deficient coverage of the femoral head, and is a known cause of hip osteoarthritis. Periacetabular osteotomy (PAO) is a surgical reorientation of the acetabulum to normalize coverage, yet its effect on joint loading is unknown. Our objective was to establish how PAO, simulated with a musculoskeletal model and probabilistic analysis, alters hip joint reaction forces (JRF) in two representative patients of two different acetabular dysplasia subgroups: anterolateral and posterolateral coverage deficiencies. PAO reorientation was simulated within the musculoskeletal model by adding three surgical degrees of freedom to the acetabulum relative to the pelvis (acetabular adduction, acetabular extension, medial translation of the hip joint center). Monte Carlo simulations were performed to generate 2000 unique PAO reorientations for each patient; from which 99% confidence bounds and sensitivity factors were calculated to assess the influence of input variability (PAO reorientation) on output (hip JRF) during gait. Our results indicate that reorientation of the acetabulum alters the lines of action of the hip musculature. Specifically, as the hip joint center was medialized, the moment arm of the hip abductor muscles was increased, which in turn increased the mechanical force-generating capacity of these muscles and decreased joint loading. Independent of subgroup, hip JRF was most sensitive to hip joint center medialization. Results from this study improve understanding of how PAO reorientation affects muscle function differently dependent upon acetabular dysplasia subgrouping and can be used to inform more targeted surgical interventions.

*Corresponding author at: Program in Physical Therapy, Washington University School of Medicine, 4444 Forest Park Ave., Suite 1101, St. Louis, MO 63108, United States. harrismi@wustl.edu (M.D. Harris).

Author contribution statement

Each author was fully involved in the conception and design of the study, data acquisition and analysis, manuscript preparation, and final approval of the submitted manuscript.

Declaration of Competing Interest

None.

Appendix A. Supplementary material

Supplementary data to this article can be found online at <https://doi.org/10.1016/j.jbiomech.2019.109464>.

Keywords

Acetabular dysplasia; Hip; Periacetabular osteotomy; Probabilistic analyses; Musculoskeletal modeling; Joint reaction force

1. Introduction

Acetabular dysplasia is characterized by abnormal acetabular geometry that results in insufficient coverage of the femoral head (Cooperman et al., 1983; Sugano et al., 1998). Coverage deficiency of the femoral head results in hip instability, as well as altered joint reaction forces (JRF) and contact stresses on the articular cartilage (Clohisy et al., 2009a; Harris et al., 2017; Henak et al., 2011). Without treatment, the abnormal geometries predispose affected patients to degenerative joint changes over time, including hip osteoarthritis (OA) (Harris-Hayes and Royer, 2011; Reijman et al., 2005).

Periacetabular osteotomy (PAO) is the most common surgical treatment for acetabular dysplasia and involves reorientation of the acetabulum relative to the femoral head (Clohisy et al., 2009b; Ganz et al., 1988). The primary objectives of PAO are to decrease pain, improve function, and establish more normal cartilage loading in an effort to delay or prevent the onset of hip OA (Clohisy et al., 2005; Leuning et al., 2001; Sanchez-Sotelo et al., 2002). For most patients, PAO establishes coverage in normal ranges (based on radiographic parameters) and improves short-term pain and function (based on patient reported outcomes) (Bogunovic et al., 2014; Clohisy et al., 2017; Igli et al., 2006). Yet, neither radiographic measures nor patient reported outcomes are representative of the mechanistic changes of PAO on hip joint loading, which is important when considering long-term cartilage integrity and the risk of OA development. Computational models suggest that intra-articular cartilage stresses are reduced following PAO (Armiger et al., 2009; Thomas-Aitken et al., 2019; Zhao et al., 2010), yet prior studies have not considered subject-specific muscle forces and joint kinematics, which also contribute to alterations in hip joint loading in acetabular dysplasia (Harris et al., 2017; Skalshoi et al., 2015). Furthermore, although the classic description of acetabular dysplasia includes general lateral coverage deficiency, it has recently been shown that patients with acetabular dysplasia include subgroups with anterolateral and posterolateral coverage deficiencies (i.e. acetabular anteversion and retroversion, respectively) (Nepple et al., 2017). Prior studies have not examined the effect of PAO on joint loading in different coverage deficiency sub-groups. This is important in the context of developing patient-specific targets for PAO reorientation that most effectively prevent or delay the onset of hip OA.

The role of the hip musculature is important for joint function and stability, primarily during single-limb weight-bearing activities when the loads within the hip are the highest (Anderson and Pandy, 2003; Neumann, 2010; Ward et al., 2010). Muscles stabilize the hip joint by generating torques that are dependent on force generation and muscle moment arms (Yanagawa et al., 2008). Inherently, as the acetabulum is reoriented with PAO, the torque generating capabilities of the surrounding musculature are altered, which will alter hip JRFs. For example, because the rectus femoris originates on the portion of the acetabulum that is

osteotomized and reoriented during PAO, its force generation capability is likely altered due to changes in its line of action (Novais et al., 2014; Peters et al., 2015). Additionally, the stabilizing torques of the primary hip abductors (gluteus medius, gluteus minimus, and tensor fascia latae) are altered following PAO due to alterations in abductor muscle moment arms (de Kleuver et al., 1998). However, to our knowledge, it is unknown if the effect of PAO on the mechanical capabilities of the surrounding hip musculature differs across dysplastic subgroups.

Probabilistic analyses provide a platform for population-based modeling by assessing the effect of individual input variability on biomechanical calculations (Laz and Browne, 2010). Monte Carlo simulation (MC) is a common probabilistic methodology that involves repeated sampling of input distributions to create output distributions (Haldar and Mahadevan, 2000). From these output distributions, the influence of input variability is most commonly quantified using confidence bounds and sensitivity factors. Applied to acetabular dysplasia, probability analysis can improve the understanding of how individual components of PAO reorientation and/or correction in each plane (rotations, translation) influence hip joint loading, and how these effects vary by coverage deficiency subgroup.

Accordingly, the objectives of this investigation were to utilize a probabilistic framework to determine the effect of simulated PAO on (1) torque generating capabilities (force, moment arms) of muscles surrounding the hip and (2) hip JRF within two coverage sub-groups (anterolateral and posterolateral) of acetabular dysplasia.

2. Methods

2.1. Participants

Acetabular coverage of the femoral head was quantified in two female patients who represented anterolateral or posterolateral coverage deficiencies found within a sample of patients with acetabular dysplasia who were recruited as part of a larger study (Table 1).

Eligibility criteria for the larger study included females, age 16–40 years, and BMI < 27 kg/m². Diagnoses of acetabular dysplasia were made by an orthopaedic surgeon (JCC) based on radiographic measures (lateral center-edge angle <20° (Wiberg, 1939) (LCEA)), anterior hip or groin pain for at least 3 months, and candidacy for PAO. Each patient provided informed consent in accordance with the Washington University School of Medicine Institutional Review Board.

Subgroups of acetabular dysplasia were defined based on coverage deficiencies in four anatomical regions of the femoral head compared to healthy, asymptomatic hips (Hansen et al., 2012; Harris et al., 2013; Nepple et al., 2017). To establish average normative values of coverage, magnetic resonance image (MRI) data from twenty-eight healthy controls who were demographically similar to the patients with dysplasia were retrospectively collected from an existing image database. Specific eligibility for controls included: females, age 16–40 years, BMI < 27 kg/m² and no radiographic evidence of acetabular dysplasia.

2.2. Coverage subgroups

MRI data were acquired from the psoas origin to the knee using a T1 weighted gradient-echo sequence with fat suppression (field of view = 480 mm; slice thickness = 1 mm) using a Siemens 3T VIDA scanner. Reconstructions of the pelvis and bilateral femurs were used to quantify coverage. Reconstructions were generated (Amira 6.5.0, FEI, Hillsboro, OR) and aligned to a neutral position using the pelvis (relative to global origin) and femur (relative to pelvis) coordinate systems, defined by Wu et al. (2002). Neutral alignment of the pelvis was defined as 7° of anterior pelvic tilt, which aligns the bilateral ASIS and pubic tubercle in the frontal plane (Arnold et al., 2010), and 0° pelvic obliquity and rotation. Neutral alignment of the femur was defined as 0° hip flexion, adduction, and rotation relative to the pelvis.

The femoral head was defined at the head-neck junction, which was identified using the zero-crossing of principal curvatures (Fig. 1a) and divided into four anatomical regions (Fig. 1b) (Hansen et al., 2012; Harris et al., 2013). Coverage of the femoral head in each region was defined as the intersections between local surface normals on the femoral head and acetabulum (PostView 2, FEBio, Salt Lake City, UT) (Fig. 1c). Anterolateral and posterolateral coverage subgroups were defined based on regional coverage that was at least 25% less than control means in each of these respective regions.

ALD, classified as a patient with anterior deficiency, had 61.5% of the control mean coverage in the anterolateral region and 103.8% of the control mean in the posterolateral region (Fig. 2). PLD, classified as a patient with posterior deficiency, had 82.6% of the control mean coverage in the anterolateral region and 61.2% of the control mean in the posterolateral region (Fig. 2).

2.3. Experimental collection and data processing

Pre-operative gait data was collected from both participants (ALD and PLD) during self-selected walking on an instrumented treadmill (Table 1). Whole-body kinematics were collected from 70 reflective markers (Vicon, Centennial, CO) and ground reaction forces (GRF) were collected from embedded force plates (Bertec, Columbus, OH), sampled at 100 Hz and 2000 Hz, respectively. Kinematic and GRF data were low-pass filtered with a 4th-order Butterworth filter (8 Hz and 30 Hz cutoff frequency, respectively). Surface electromyography was recorded ($F_s = 2000$ Hz) from bipolar Ag/AgCl surface electrodes (inter-electrode distance: 1 cm; CMRR > 100 db) (Vermed, Buffalo, NY) placed on the rectus femoris, biceps femoris long head, vastus lateralis, and medial gastrocnemius according to SENIAM guidelines (Merletti and Hermens, 2000) and used for model validation (see Supplementary Material). We chose these muscles based on their large superficial area, which reduces potential EMG signal crosstalk from surrounding muscles. Because the purpose of the control group was only to establish normative coverage values, no gait data was collected from this group.

2.4. Musculoskeletal model

An existing, generic OpenSim musculoskeletal model (Lai et al., 2017) was personalized for the two representative patients. Subject-specific changes included: (1) substituting the pelvis and femur geometries in place of the generic OpenSim geometry, (2) establishing subject-

specific bilateral HJC defined as the center of spheres fit to the patient's femoral heads (Harris et al., 2017), and (3) updating the hip musculature origin and insertion sites within the model using the MR images and the subject-specific bony geometry. The remaining segment geometries were generic and were scaled according to each patient's anthropometric measurements using markers placed on anatomical landmarks.

Simulated PAO was accomplished by resecting the acetabulum in Amira (v6.5, FEI, Hillsboro, OR) and including three additional degrees of freedom (DOF) to represent common degrees of surgical reorientation (Clohisy et al., 2006). First, acetabular resection was accomplished using planar cuts defined by landmarks on the pelvis: (1) axial slice at the most anterior prominence of the anterior inferior iliac spine (AIIS), (2) the most lateral prominence of the ischium, and (3) midpoint of the pubis ramus. Three DOF were added within the OpenSim model to allow for rotation/translation of the resected acetabulum (child segment) relative to the pelvis (parent segment). These DOFs included: (1) acetabular adduction: frontal plane rotation of the acetabulum (to address lateral coverage deficiency), (2) acetabular extension: sagittal plane rotation of the acetabulum (to address anterior/posterior coverage deficiency), and (3) medial translation of the hip joint center (Fig. 3). The origin of the rectus femoris was located on the AIIS; therefore, its line of action and moment arm were explicitly dependent upon the reorientation of the acetabulum (extension/adduction) within the simulated PAO, while the moment arms of all muscles were indirectly dependent upon the medialization of the hip joint center.

One gait cycle (symptomatic limb heel strike to symptomatic limb heel strike) was used for analysis. A residual reduction algorithm was used to maintain dynamic consistency between experimental and model estimated data (joint angles, segmental mass distribution) (Delp et al., 2007). Static optimization was used to estimate muscle forces by solving for the net joint moments as individual muscle forces while minimizing the sum of squared muscle activations surrounding the joint (Anderson and Pandy, 2001). Finally, anterior/posterior (A/P), superior/inferior (S/I), and medial/lateral (M/L) components of the hip JRF, and the resultant JRF were determined on the symptomatic hip (Steele et al., 2012). Model validation was accomplished by (1) minimizing residual forces and moments in accordance with OpenSim recommendations (on SimTK.org), (2) comparing onset/offset timings of experimental electromyography to model predicted activations (Hicks et al., 2015), and (3) comparing hip JRF to previously published data in a similar population (Harris et al., 2017) (see Supplementary Material).

2.5. Probabilistic analysis

Two thousand Monte Carlo (MC) simulations (Halder and Mahadevan, 2000), were used to assess the impact of simulated PAO DOF reorientation (input distributions) on the hip JRF (output distributions). 2000 simulations were chosen based on a convergence criteria of similar methodologies that states that the means and standard deviations of the output (hip JRF) lay within 1% of each final mean and standard deviations over the last 100 simulations (Myers et al., 2015; Navacchia et al., 2016; Valente et al., 2013). A custom interface using the OpenSim/Matlab API was developed to perturb the baseline model. PAO reorientation was randomly generated from DOF input distributions that were derived from a database of

surgical reports from PAOs performed by the same orthopaedic surgeon (JCC) (Clohisy et al., 2007). Specifically, distribution ranges included: acetabular adduction (15° – 51°), acetabular extension (-25 – 52°), and hip joint center medialization (0–23 mm). Within each trial of the MC simulation, the randomly generated PAO reorientation was combined with the deterministic inputs (pre-operative gait data for each patient) and used to solve for the hip JRFs.

Output distributions from the MC simulations were used to determine the influence of PAO on hip JRF using confidence bounds and sensitivity factors. Confidence bounds quantify the *overall* impact of variability in each PAO degree of freedom on biomechanical outputs by determining a range (e.g. bound) associated with a specific probability (99%) of the output variable. Specifically, 0.5–99.5% confidence bounds were calculated for the A/P, S/I, M/L, and the resultant JRF, as well as muscle forces surrounding the hip in early stance (JRF1: ~14% gait cycle) and in terminal stance (JRF2: ~47% gait cycle). The bound size of the hip JRFs and muscle forces (rectus femoris (RECFEM) and primary hip abductors (gluteus medius (GMED) anterior/middle/posterior, gluteus minimus (GMIN) anterior/middle/posterior, and the tensor fascia latae (TFL)) were calculated across the entire gait cycle and compared across each participant (ALD and PLD) at JRF1 and JRF2. Sensitivity factors quantify the *individual* effect of altering individual PAO DOFs on hip JRFs, and therefore indicate how sensitive hip JRFs are to each specific PAO DOF. Sensitivity factors were calculated by correlating the individual PAO DOFs to the JRFs and muscle moment arms using Pearson product-moment correlation coefficients (r) at JRF1 and JRF2. Sensitivity factors were categorized as weak ($0.2 < r < 0.4$), moderate ($0.4 < r < 0.6$), or strong ($0.6 < r < 1.0$) (Gaffney et al., 2017; Myers et al., 2015). Positive sensitivity factors indicate a reduction in JRF.

3. Results

3.1. Confidence bounds

For each patient, acetabular reorientation had the largest impact on the S/I and resultant hip JRFs (Fig. 4a), yet the timing of influence during early (JRF1) and late (JRF2) stance differed between patients (Fig. 4b). For ALD, bounds for the resultant JRF were substantially larger at JRF2 (3.49 xBW) than JRF1 (2.46 xBW); however, for PLD, the bounds for the resultant JRF were larger at JRF1 (1.61 xBW) than JRF2 (1.35 xBW) (Fig. 4b). In addition, PAO reorientation had a larger influence on ALD than PLD, as indicated by the relative bound sizes (Fig. 4b).

3.2. Sensitivity factors

Statistically significant sensitivity factors (correlations) for hip JRF and all simulated PAO reorientation DOF were identified in both early and late stance for both patients (Fig. 5). At JRF1, the resultant JRF was moderately sensitive to acetabular extension (ALD: $r = 0.58$ [0.56 0.61]; PLD: $r = 0.48$ [0.44 0.51]); while at JRF2, the A/P JRF was moderately sensitive to acetabular extension (ALD: $r = 0.48$ [0.45 0.51]; PLD: $r = 0.55$ [0.52 0.58]). For PLD, hip JRF was moderately sensitive to acetabular adduction at JRF1 in the S/I, M/L, and resultant directions ($r = 0.50$ [0.47 0.54], $r = 0.32$ [0.28 0.63], and $r = 0.49$ [0.45 0.52],

respectively); yet for ALD, only the M/L JRF at JRF1 was sensitive to acetabular adduction ($r = 0.44$ [0.41 0.48]). For both patients, at JRF1 and JRF2, all components of hip JRF were moderately or strongly sensitive to hip joint center medialization, which resulted in a decrease in JRF, with the strongest sensitivity being in the resultant force at JRF2 (ALD: $r = 0.97$ [0.96 0.98]; PLD: $r = 0.98$ [0.97 0.99]).

3.3. Muscle force and moment arms

Acetabular reorientation had the largest influence on muscle force generation of the RECFEM during early stance and TFL during late stance for both patients (Fig. 6). RECFEM moment arms were sensitive to acetabular adduction and extension reorientation, while the moment arms of the primary abductors were sensitive to hip joint center medialization (Table 2).

4. Discussion

The objective of this investigation was to assess the influence of PAO reorientation on hip JRF in patients representing two coverage subgroups of acetabular dysplasia. Using a probabilistic analysis, we established that the hip JRF in both patients was most sensitive to medialization of the hip joint center, while the influence of PAO reorientation differed across patients. Identifying the differences in sensitivity of joint loading to PAO reorientation across acetabular dysplasia subgroups is critical to understanding the optimal, patient-specific alignment in the context of joint loading.

Our results indicate that, independent of subgroup, hip JRF was most sensitive to medialization of the hip joint center. Specifically, all components of the JRF were significantly reduced in both early and late stance when the hip joint center was medialized. Due to the altered bony geometry in acetabular dysplasia, the hip joint center is more lateral compared to healthy hips, which reduces abductor moment arms (Maquet, 1999; Clohisy et al., 2004). In order to produce the abductor torque required to stabilize the body during single limb support, the abductor muscles must increase their force production, which results in increased medially directed JRFs (Harris et al., 2017). Medializing the hip joint center during PAO decreases the external gravitational moment arm between joint center and body center of mass and leads to a reduction of JRFs. To our knowledge, these results are the first to establish empirical evidence pertaining to the direct effect of hip joint center medialization on a reduction of hip joint loading in acetabular dysplasia.

Understanding the differing influence of PAO on hip joint loading between subgroups of acetabular dysplasia is important for informing optimal surgical reorientation. Our results indicate that the influence of PAO was larger in late stance (JRF2) for the patient with anterior coverage deficiency, as evidenced by the larger bound size. In late stance, the extended position of the hip results in anteriorly directed joint loads. This is of clinical importance given that cartilage damage commonly occurs in the anterolateral region of the acetabulum (Henak et al., 2014; Klaue et al., 1991; Noguchi et al., 1999; Tamura et al., 2012). Contrarily, for the patient with posterior coverage deficiency, the influence of PAO was greater in early stance (JRF1). During loading, the hip JRFs are directed more posteriorly, which may indicate that patients with posterior coverage deficiency may be

more susceptible to concurrent posterior joint damage. Thus, PAO reorientation has important influences on joint loading that vary throughout the gait cycle dependent on coverage type.

Lateral coverage deficiency is common in most cases of acetabular dysplasia, and therefore likely prioritized in PAO through acetabular adduction reorientation. For PLD, who had substantial lateral coverage deficiency, the magnitude of superior, medial, and resultant hip JRF was moderately sensitive to acetabular adduction, indicating a reduction in total joint load as lateral coverage increased. Additionally, in both patients, the medially directed hip JRF in early stance, which has been shown to be larger in patients with acetabular dysplasia (pre-PAO) (Harris et al., 2017), was moderately sensitive (reduced) to increased acetabular adduction. We attribute the lack of strong sensitivity of hip JRF to acetabular adduction to the relatively small change in adductor moment arm of the rectus femoris and no effect on the moment arm of the primary abductors. Additionally, we also attribute this finding to modeling each DOF of reorientation independent of one another in the current model. Acetabular adduction likely coincides with medialization of the hip joint center. Therefore, when adduction reorientation is coupled with hip joint center medialization, it would likely strengthen the sensitivity of reduction in hip JRF to PAO reorientation.

Hip JRFs represent joint loads that are largely muscle-driven, and JRF alterations are primarily attributed to alterations in the force generating capacity of the hip musculature (Correa et al., 2010). Similar to all PAO techniques, the origin and insertion sites of the primary abductors were not changed. Therefore, alterations in joint loading due to force generated by the abductor musculature is solely attributed to changes in the moment arms of these muscles relative to the hip joint center. However, there is a disparity amongst surgical techniques regarding the preservation of the rectus femoris origin. Traditional PAO techniques involve takedown of the direct and reflected heads of the rectus femoris tendon to allow for an anterior capsulotomy (Ganz et al., 1988; Hussell et al., 1999), which would alter both the path and overall function of the muscle. However, recent surgical refinements recommend maintaining the attachment of the rectus femoris (Novais et al., 2014; Peters et al., 2015), in an effort to improve post-operative hip flexor strength (Sucato et al., 2010). The current simulation is representative of the recommended surgical refinement technique, as the rectus femoris originated on the osteotomized portion of the acetabulum and was maintained (i.e. its origin site did not change relative to the bone during reorientation). Therefore, changes in joint loading attributed to alterations in force generation of the rectus femoris are attributed to changes in length, line of action, and moment arm relative to the hip joint center. To our knowledge, biomechanical data comparing rectus femoris tendon sparing versus non-sparing does not exist. Future work could implement similar probabilistic analyses to establish the differences in sensitivity of joint loading to rectus sparing versus non-sparing approaches.

It is important to note that this investigation included two representative patients with acetabular dysplasia. Although this investigation implemented a probabilistic analysis, which is robust tool that uses population-based probabilistic input distributions, the deterministic inputs (kinematics, ground reaction forces) remain specific to each representative patient. Therefore, because these deterministic inputs have a direct effect on

muscle-driven joint loading and are known to vary across subjects, our results should be interpreted with caution when generalizing to the larger population of patients with acetabular dysplasia. Due to the robustness of probabilistic analyses, previous investigations implementing similar methodologies have utilized similar sample sizes (Myers et al., 2015, 2019; Navacchia et al., 2016; Smith et al., 2019; Valente et al., 2013). However, future work is needed to establish if large differences in muscle-driven joint loading across subgroups of acetabular dysplasia exist and if these are due to changes in deterministic inputs such as hip kinematics or pre-PAO lateral acetabular coverage.

Several limitations of this study exist that should be considered. First, as mentioned above, input distributions were modeled from independent Gaussian distributions. Although we anticipate there to be relationships between degrees of reorientation (specifically between acetabular adduction and medialization of the hip joint center), we chose to model the input distributions independently to isolate their individual effects on joint loading. Because acetabular adduction and hip joint center medialization both resulted in decreased hip JRF, we believe that our results would be stronger if modeled dependently. Second, the probabilistic analyses did not incorporate deterministic inputs (kinematics, external forces) from post-surgical movements, but instead from pre-surgical movements. Movement patterns may change in some patients after PAO (Jacobsen et al., 2014; Pedersen et al., 2006; Sucato et al., 2010); thus, we cannot determine the influence of post-surgical movement differences on our findings. Third, proximal femoral deformities that exist in this population (Clohisy et al., 2009a; Gaffney et al., 2019; Wells et al., 2017) were not considered in this simulated PAO. While femoral deformities may be important to joint mechanics, current surgical decision making about the amount and direction of PAO reorientation is primarily based on acetabular geometry. Fourth, this investigation only included female participants, because females comprise 72–80% of patients presenting with symptoms of acetabular dysplasia (Bach et al., 2002; Chan et al., 1997; Nunley et al., 2011). While males were not included, if they present with similar acetabular coverage deficiencies and movement patterns, results from the current study may also apply to them. Finally, the findings of this study are dependent upon the PAO surgical technique simulated in our models, which were described by Clohisy et al. (2006). Surgical variations, such as rectus femoris detachment, or reorientation of the sartorius attachment on the anterior superior iliac spine may influence the sensitivity of hip JRFs.

In conclusion, our findings suggest acetabular reorientation reduces the magnitude of hip JRF, with the strongest sensitivity due to medialization of the hip joint center. However, the influence of PAO differed in timing between the two patients representing different coverage deficiencies (anterior vs. posterior coverage deficiency), which we attribute to the direction of the JRF within the acetabulum relative to the region of coverage deficiency. Results from this study can improve understanding of how PAO reorientation affects muscle-driven joint loading dependent upon bony morphology and can be used to inform more targeted surgical interventions.

Supplementary Material

Refer to Web version on PubMed Central for supplementary material.

Acknowledgements

This project was supported by the National Institutes of Health (Grant Numbers: T32HD007434, K01AR072072, P30AR074992, F32AR075349), the L'Oréal USA For Women in Science Fellowship, and the Caroline Lottie Hardy Charitable Trust. Additional support was obtained from the Curing Hip Disease Fund (JCC). We thank Jacqueline Foody and Molly Shepherd for their assistance in data processing and segmentation.

References

- Anderson FC, Pandy MG, 2003 Individual muscle contributions to support in normal walking. *Gait Posture* 17, 159–169. 10.1016/S0966-6362(02)00073-5. [PubMed: 12633777]
- Anderson FC, Pandy MG, 2001 Static and dynamic optimization solutions for gait are practically equivalent. *J. Biomech* 34, 153–161. [PubMed: 11165278]
- Armiger RS, Armand M, Tallroth K, Lepistö J, Mears SC, 2009 Three-dimensional mechanical evaluation of joint contact pressure in 12 periacetabular osteotomy patients with 10-year follow-up. *Acta Orthop.* 80, 155–161. 10.3109/17453670902947390. [PubMed: 19404795]
- Arnold EM, Ward SR, Lieber RL, Delp SL, 2010 A model of the lower limb for analysis of human movement. *Ann. Biomed. Eng* 38, 269–279. [PubMed: 19957039]
- Bache CE, Clegg J, Herron M, 2002 Risk factors for developmental dysplasia of the hip: ultrasonographic findings in the neonatal period. *J. Pediatr. Orthop. B* 11, 212–218. [PubMed: 12089497]
- Bogunovic L, Hunt D, Prather H, Schoenecker PL, Clohisy JC, 2014 Activity tolerance after periacetabular osteotomy. *Am. J. Sports Med* 42, 1791–1795. 10.1177/0363546514535906. [PubMed: 24914031]
- Chan A, McCaul KA, Cundy PJ, Haan EA, Byron-Scott R, 1997 Perinatal risk factors for developmental dysplasia of the hip. *Arch. Dis. Child. Fetal Neonatal Ed* 76, 94–100. 10.1136/fn.76.2.F94.
- Clohisy JC, Ackerman J, Baca G, Baty J, Beaulé PE, Kim YJ, Millis MB, Podeszwa DA, Schoenecker PL, Sierra RJ, Sink EL, Sucato DJ, Trousdale RT, Zaltz I, 2017 Patient-reported outcomes of periacetabular osteotomy from the prospective ANCHOR cohort study. *J. Bone Jt. Surg. - Am* 99, 33–41. 10.2106/JBJS.15.00798.
- Clohisy JC, Barrett SE, Gordon JE, Delgado ED, Schoenecker PL, 2006 Periacetabular osteotomy in the treatment of severe acetabular dysplasia. Surgical technique. *J. Bone Joint Surg. Am* 88 (Suppl 1), 65–83. 10.2106/00004623-200603001-00007. [PubMed: 16510801]
- Clohisy JC, Barrett SE, Gordon JE, Delgado ED, Schoenecker PL, 2005 Periacetabular osteotomy for the treatment of severe acetabular dysplasia. *J. Bone Jt. Surg* 87, 254–259. 10.2106/JBJS.D.02093.
- Clohisy JC, Barrett SE, Gordon JE, Delgado ED, Schoenecker PL, 2004 Medial translation of the hip joint center associated with the Bernese periacetabular osteotomy. *Iowa Orthop. J* 24, 43–48. [PubMed: 15296205]
- Clohisy JC, Nunley RM, Carlisle JC, Schoenecker PL, 2009a Incidence and characteristics of femoral deformities in the dysplastic hip. *Clin. Orthop. Relat. Res* 467, 128–134. 10.1007/s11999-008-0481-3. [PubMed: 19034600]
- Clohisy JC, Nunley RM, Curry MC, Schoenecker PL, 2007 Periacetabular osteotomy for the treatment of acetabular dysplasia associated with major aspherical femoral head deformities. *J. Bone Jt. Surg. - Ser. A* 89, 1417–1423. 10.2106/JBJS.F.00493.
- Clohisy JC, Schutz AL, St. John L, Schoenecker PL, Wright RW, 2009b Periacetabular osteotomy: a systematic literature review. *Clin. Orthop. Relat. Res* 467, 2041–2052. 10.1007/s11999-009-0842-6. [PubMed: 19381741]
- Cooperman DR, Wallensten R, Stulberg SD, 1983 Acetabular dysplasia in the adult. *Clin. Orthop. Relat. Res*, 79–85 <https://doi.org/0009-921X/83/0500/079>. [PubMed: 6839611]
- Correa TA, Crossley KM, Kim HJ, Pandy MG, 2010 Contributions of individual muscles to hip joint contact force in normal walking. *J. Biomech* 43, 1618–1622. 10.1016/j.jbiomech.2010.02.008. [PubMed: 20176362]

- de Kleuver M, Huiskes R, Kauer JM, Veth RP, 1998 Three-dimensional displacement of the hip joint after triple pelvic osteotomy. A postmortem radiostereometric study. *Acta Orthop. Scand* 69, 585–589. 10.3109/17453679808999260. [PubMed: 9930102]
- Delp SL, Anderson FC, Arnold AS, Loan P, Habib A, John CT, Guendelman E, Thelen DG, 2007 OpenSim: Open-source Software to Create and Analyze Dynamic Simulations of Movement.
- Gaffney BMM, Christiansen CL, Murray AM, Myers CA, Laz PJ, Davidson BS, 2017 The effects of prosthesis inertial parameters on invertebral dynamics: a probabilistic analysis. *ASME J. Verif. Validation Uncertain. Quantif* 2, 1–8. 10.1115/1.4038175.
- Gaffney BMM, Hillen TJ, Nepple JJ, Clohisey JC, Harris MD, 2019 Statistical shape modeling of femur shape variability in female patients with hip dysplasia. *J. Orthop. Res* 37, 665–673. 10.1002/jor.24214. [PubMed: 30656719]
- Ganz R, Klaue K, Vinh TS, Mast JW, 1988 A new periacetabular osteotomy for the treatment of hip dysplasias. *Clin. Orthop. Relat. Res.* 26–36
- Haldar A, Mahadevan S, 2000 *Probability, Reliability, and Statistical Methods in Engineering Design.* John Wiley & Sons. Inc., New York, NY.
- Halder A, Mahadevan S, 2000 *Probability, Reliability and Statistical Methods in Engineering and Design.* Wiley, New York, NY.
- Hansen BJ, Harris MD, Anderson LA, Peters CL, Weiss JA, Anderson AE, 2012 Correlation between radiographic measures of acetabular morphology with 3D femoral head coverage in patients with acetabular retroversion. *Acta Orthop.* 83, 233–239. 10.3109/17453674.2012.684138. [PubMed: 22553905]
- Harris-Hayes M, Royer NK, 2011 Relationship of acetabular dysplasia and femoroacetabular impingement to hip osteoarthritis: a focused review. *PM R* 3, 1055–1067.e1. 10.1016/j.pmrj.2011.08.533. [PubMed: 22108232]
- Harris MD, MacWilliams BA, Bo Foreman K, Peters CL, Weiss JA, Anderson AE, 2017 Higher medially-directed joint reaction forces are a characteristic of dysplastic hips: a comparative study using subject-specific musculoskeletal models. *J. Biomech* 54, 80–87. 10.1016/j.jbiomech.2017.01.040. [PubMed: 28233552]
- Harris MD, Reese SP, Peters CL, Weiss JA, Anderson AE, 2013 Three-dimensional quantification of femoral head shape in controls and patients with cam-type femoroacetabular impingement. *Ann. Biomed. Eng* 41, 1162–1171. 10.1007/s10439-013-0762-1. [PubMed: 23413103]
- Henak CR, Abraham CL, Anderson AE, Maas SA, Ellis BJ, Peters CL, Weiss JA, 2014 Patient-specific analysis of cartilage and labrum mechanics in human hips with acetabular dysplasia. *Osteoarthr. Cartil* 22, 210–217. 10.1016/j.joca.2013.11.003. [PubMed: 24269633]
- Henak CR, Ellis BJ, Harris MD, Anderson AE, Peters CL, Weiss JA, 2011 Role of the acetabular labrum in load support across the hip joint. *J. Biomech* 44, 2201–2206. 10.1016/j.jbiomech.2011.06.011. [PubMed: 21757198]
- Hicks JL, Uchida TK, Seth A, Rajagopal A, Delp S, 2015 Is my model good enough? Best practices for verification and validation of musculoskeletal models and simulations of human movement. *J. Biomech. Eng* 137 10.1115/1.4029304.
- Hussell J, Mast J, Mayo K, Howie D, Ganz R, 1999 A comparison of different surgical approaches for the periacetabular osteotomy. *Clin. Orthop. Relat. Res* 363, 64–72.
- Igli A, Antoli V, Kralj-Igli V, Mavri B, Kralj M, 2006 The Bernese periacetabular osteotomy: clinical, radiographic and mechanical 7–15-year follow-up of 26 hips. *Acta Orthop.* 76, 833–840. 10.1080/17453670510045453.
- Jacobsen JS, Nielsen DB, Sørensen H, Søballe K, Mechlenburg I, 2014 Joint kinematics and kinetics during walking and running in 32 patients with hip dysplasia 1 year after periacetabular osteotomy. *Acta Orthop.* 85, 592–599. 10.3109/17453674.2014.960167. [PubMed: 25191933]
- Klaue K, Durnin C, Ganz R, 1991 The acetabular rim syndrome. A clinical presentation of dysplasia of the hip. *Bone Joint J.* 73, 423–429.
- Lai AKM, Arnold AS, Wakeling JM, 2017 Why are antagonist muscles coactivated in my simulation? a musculoskeletal model for analysing human locomotor tasks. *Ann. Biomed. Eng* 45, 2762–2774. 10.1007/s10439-017-1920-7. [PubMed: 28900782]

- Laz PJ, Browne M, 2010 A review of probabilistic analysis in orthopaedic biomechanics. *Proc. Inst. Mech. Eng. Part H J. Eng. Med* 224, 927–943.
- Leuning M, Siebenrock KA, Ganz R, 2001 Rationale of periacetabular osteotomy and background. *Work. J. Bone Jt. Surg* 83-A, 438–448. 10.1016/j.mporth.2012.04.006.
- Maquet P, 1999 Biomechanics of hip dysplasia. *Acta Orthop. Belg* 10.1007/978-3-642-50960-5.
- Merletti R, Hermens H, 2000 Introduction to the special issue on the SENIAM European Concerted Action. *J. Electromyogr. Kinesiol* 10, 283–286. [PubMed: 11018437]
- Myers C.a., Laz PJ, Shelburne KB, Davidson BS, 2015 A probabilistic approach to quantify the impact of uncertainty propagation in musculoskeletal simulations. *Ann. Biomed. Eng* 43, 1098–1111. [PubMed: 25404535]
- Myers CA, Laz PJ, Shelburne KB, Judd DL, Winters JD, Stevens-Lapsley JE, Davidson BS, 2019 Simulated hip abductor strengthening reduces peak joint contact forces in patients with total hip arthroplasty. *J. Biomech* 10.1016/j.jbiomech.2019.06.003.
- Navacchia A, Myers CA, Rullkoetter PJ, Shelburne KB, 2016 Prediction of in vivo knee joint loads using a global probabilistic analysis. *J. Biomech. Eng* 138, 031002.
- Nepple JJ, Wells J, Ross JR, Bedi A, Schoenecker PL, Clohisy JC, 2017 Three patterns of acetabular deficiency are common in young adult patients with acetabular dysplasia. *Clin. Orthop. Relat. Res* 475, 1037–1044. 10.1007/s11999-016-5150-3. [PubMed: 27830486]
- Neumann DA, 2010 Kinesiology of the hip: a focus on muscular actions. *J. Orthop. Sport. Phys. Ther* 40, 82–94. 10.2519/jospt.2010.3025.
- Noguchi Y, Miura H, Takasugi SI, Iwamoto Y, 1999 Cartilage and labrum degeneration in the dysplastic hip generally originates in the anterosuperior weight-bearing area: an arthroscopic observation. *Arthroscopy* 15, 496–506. 10.1053/ar.1999.v15.015049. [PubMed: 10424553]
- Novais EN, Kim YJ, Carry PM, Millis MB, 2014 The Bernese periacetabular osteotomy: is transection of the rectus femoris tendon essential?. *Clin. Orthop. Relat. Res* 472, 3142–3149. 10.1007/s11999-014-3720-9. [PubMed: 25053288]
- Nunley RM, Prather H, Hunt D, Schoenecker PL, Clohisy JC, 2011 Clinical presentation of symptomatic acetabular dysplasia in skeletally mature patients. *J. Bone Joint Surg. Am* 93 (Suppl 2), 17–21. 10.2106/JBJS.J.01735. [PubMed: 21543683]
- Pedersen ENG, Alkjær T, Søballe K, Simonsen EB, 2006 Walking pattern in 9 women with hip dysplasia 18 months after periacetabular osteotomy. *Acta Orthop.* 77, 203–208. 10.1080/17453670610045920. [PubMed: 16752280]
- Peters CL, Erickson JA, Anderson MB, Anderson LA, 2015 Preservation of the rectus femoris origin during periacetabular osteotomy does not compromise acetabular reorientation. *Clin. Orthop. Relat. Res* 473, 608–614. 10.1007/s11999-014-3837-x. [PubMed: 25091227]
- Reijman M, Hazes JMW, Pols HAP, Koes BW, Bierma-Zeinstra SMA, 2005 Acetabular dysplasia predicts incident osteoarthritis of the hip: the Rotterdam study. *Arthritis Rheum.* 52, 787–793. 10.1002/art.20886. [PubMed: 15751071]
- Sanchez-Sotelo J, Trousdale RT, Berry DJ, Cabanela ME, 2002 Surgical treatment of developmental dysplasia of the hip in adults: 1. Nonarthroplasty options. *J. Am. Acad. Orthop. Surg* 10, 321–333. [PubMed: 12374483]
- Skalshoi O, Iversen CH, Nielsen DB, Jacobsen J, Mechlenburg I, Soballe K, Sorensen H, 2015 Walking patterns and hip contact forces in patients with hip dysplasia. *Gait Posture* 42, 529–533. 10.1016/j.gaitpost.2015.08.008. [PubMed: 26365370]
- Smith CR, Brandon SCE, Thelen DG, 2019 Can altered neuromuscular coordination restore soft tissue loading patterns in anterior cruciate ligament and menisci deficient knees during walking?. *J. Biomech* 82, 124–133. 10.1016/j.jbiomech.2018.10.008. [PubMed: 30420173]
- Steele KM, Demers MS, Schwartz MH, Delp SL, 2012 Compressive tibiofemoral force during crouch gait. *Gait Posture* 35, 556–560. 10.1016/j.gaitpost.2011.11.023. [PubMed: 22206783]
- Sucato DJ, Tulchin K, Shrader MW, Delarocha A, Gist T, Sheu G, 2010 Gait, hip strength and functional outcomes after a ganz periacetabular osteotomy for adolescent hip dysplasia. *J. Pediatr. Orthop* 30, 344–350. 10.1097/BPO.0b013e3181d9bfa2. [PubMed: 20502234]

- Sugano N, Noble PC, Kamaric E, Salama JK, Ochi T, Tullos HS, 1998 The morphology of the femur in developmental dysplasia of the hip. *J. Bone Joint Surg. Br* 80, 711–719. 10.1302/0301-620X.80B4.8319. [PubMed: 9699842]
- Tamura S, Nishii T, Shiomi T, Yamazaki Y, Murase K, Yoshikawa H, Sugano N, 2012 Three-dimensional patterns of early acetabular cartilage damage in hip dysplasia; a high-resolutional CT arthrography study. *Osteoarthr. Cartil* 20, 646–652. 10.1016/j.joca.2012.03.015. [PubMed: 22469852]
- Thomas-Aitken HD, Goetz JE, Dibbern KN, Westermann RW, Willey MC, Brown TS, 2019 Patient age and hip morphology alter joint mechanics in computational models of patients with hip dysplasia. *Clin. Orthop. Relat. Res* 1 10.1097/CORR.0000000000000621.
- Valente G, Taddei F, Jonkers I, 2013 Influence of weak hip abductor muscles on joint contact forces during normal walking: Probabilistic modeling analysis. *J. Biomech* 46, 2186–2193. [PubMed: 23891175]
- Ward SR, Winters TM, Blemker SS, 2010 The architectural design of the gluteal muscle group: implications for movement and rehabilitation. *J. Orthop. Sport. Phys. Ther* 40, 95–102. 10.2519/jospt.2010.3302.
- Wells J, Nepple JJ, Crook K, Ross JR, Bedi A, Schoenecker P, Clohisy JC, 2017 Femoral morphology in the dysplastic hip: three-dimensional characterizations With CT. *Clin. Orthop. Relat. Res* 475, 1045–1054. 10.1007/s11999-016-5119-2. [PubMed: 27752989]
- Wiberg G, 1939 The anatomy and roentgenographic appearance of a normal hip joint. *Acta Chir. Scand* 83, 7–38.
- Wu G, Siegler S, Allard P, Kirtley C, Leardini A, Rosenbaum D, Whittle M, D’Lima D, Cristofolini L, Witte H, Schmid O, Stokes I, 2002 ISB recommendation on definitions of joint coordinate systems of various joints for the reporting of human joint motion-part I: ankle, hip, and spine. *J. Biomech* 35, 543–548. [PubMed: 11934426]
- Yanagawa T, Goodwin CJ, Shelburne KB, Giphart JE, Torry MR, Pandy MG, 2008 Contributions of the individual muscles of the shoulder to glenohumeral joint stability during abduction. *J. Biomech. Eng* 130,. 10.1115/1.2903422021024.
- Zhao X, Chosa E, Totoribe K, Deng G, 2010 Effect of periacetabular osteotomy for acetabular dysplasia clarified by three-dimensional finite element analysis. *J. Orthop. Sci* 15, 632–640. 10.1007/s00776-010-1511-z. [PubMed: 20953924]

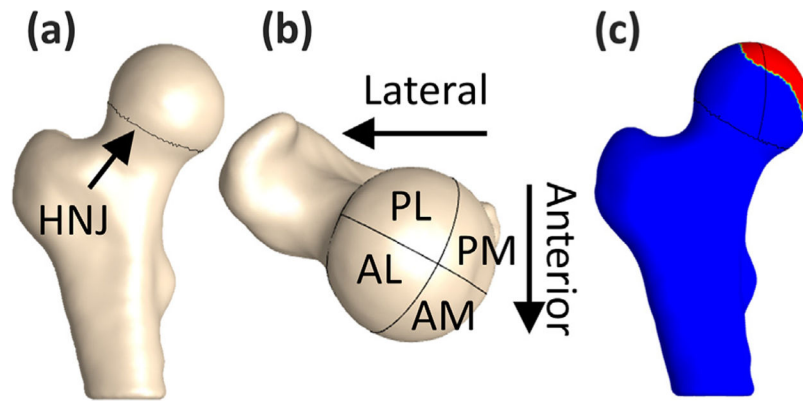


Fig. 1. (a) Femoral head defined at the head-neck junction (HNJ), (b) four anatomical regions of the femoral head: anterolateral (AL), anteromedial (AM), posterolateral (PL), and posteromedial (PM), and (c) the region of the femoral head covered by the acetabulum (red).

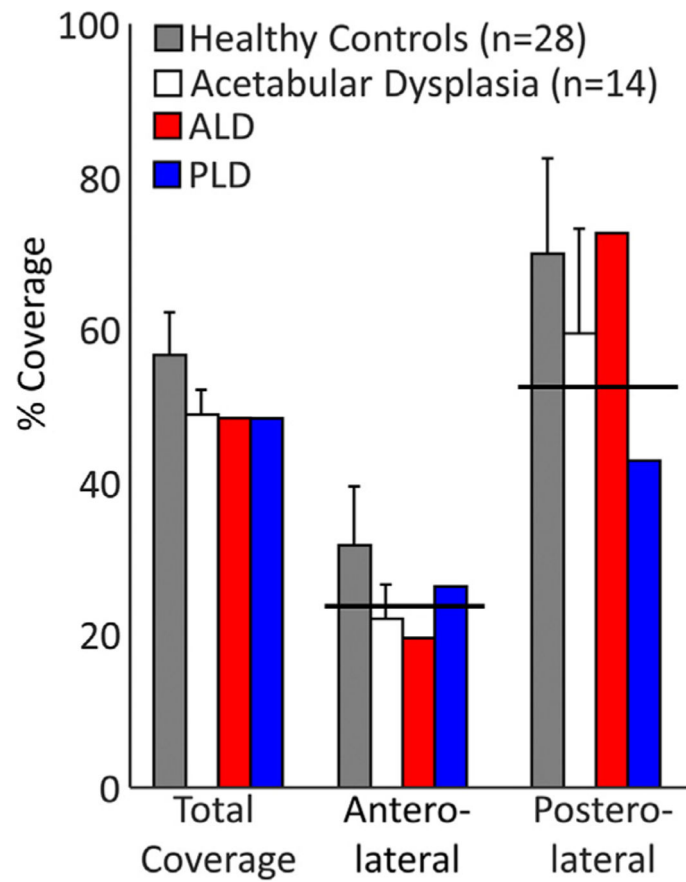


Fig. 2.

Percent femoral head coverage between healthy controls (HC), a larger sample of patients with acetabular dysplasia (mean \pm SD), and the two acetabular dysplasia patients within each anatomic region. Black solid line indicates the threshold level used to define coverage subgroups (25% less than the control mean).

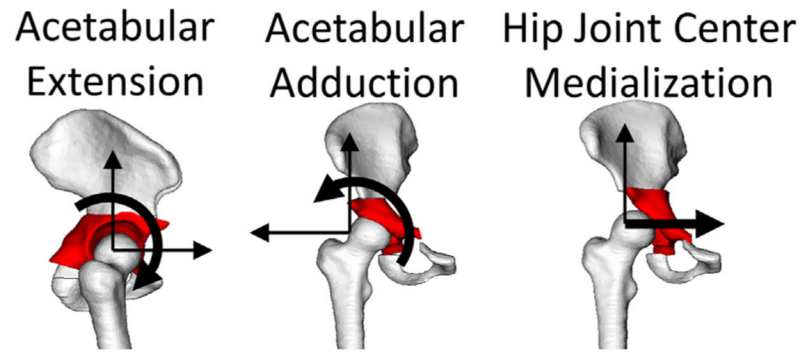


Fig. 3.

Simulated PAO was accomplished by including three additional degrees of freedom of the acetabulum relative to the femoral head: extension, adduction, and hip joint center medialization. Medialization was defined as the change between preoperative and postoperative distance between the ilioischial line and the medial aspect of the femoral head (Clohisy et al., 2004).

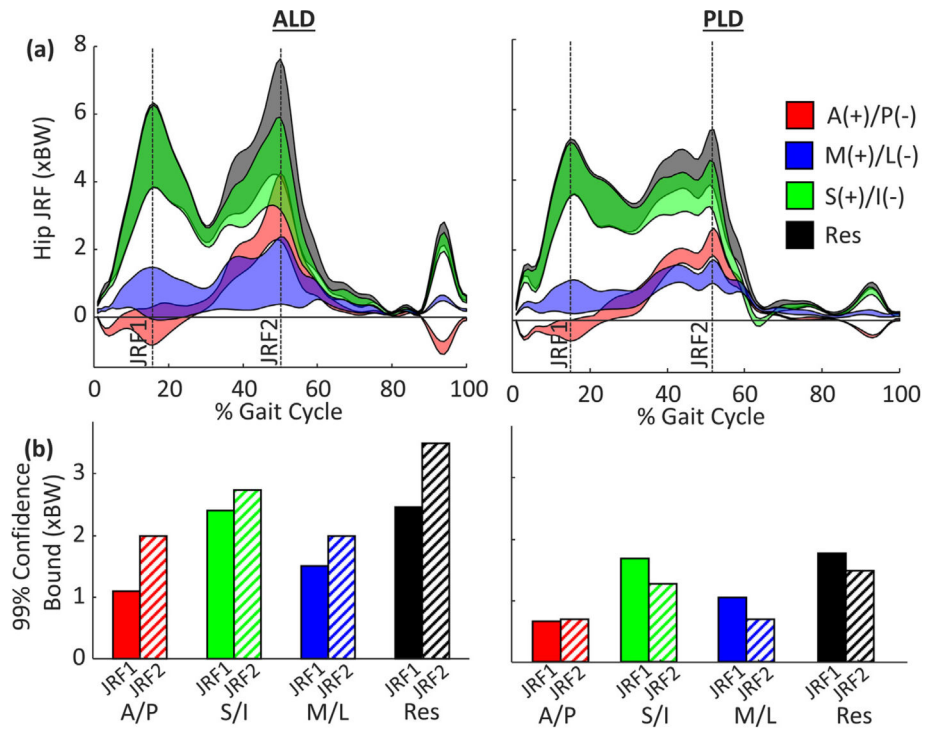


Fig. 4. (a) 99% confidence bounds of hip JRF in the A/P (red), S/I (green), M/L (blue), and resultant (grey) directions for the anterolateral (ALD) and posterolateral (PLD) coverage deficient patients and (b) confidence bound of hip JRF during early stance (JRF1 – solid) and late stance (JRF2 – hashed).

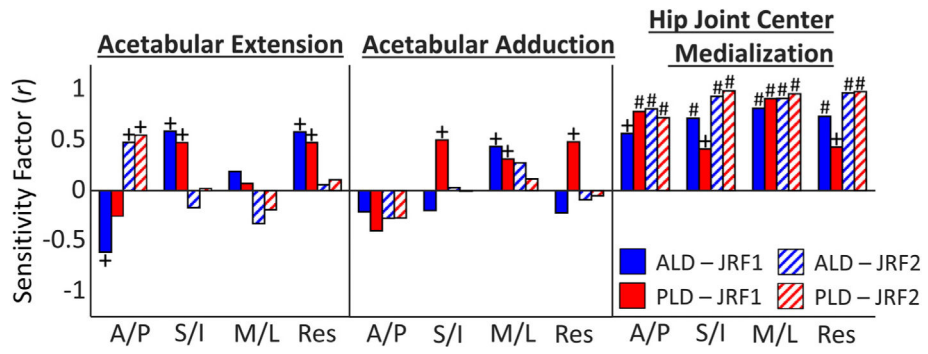


Fig. 5. Sensitivity factors (r) between JRF components at JRF1 and JRF2, and PAO reorientation (note: a positive sensitivity factor indicates a decrease in JRF magnitude). +indicates moderate sensitivity ($0.4 < r < 0.6$) and #indicates strong sensitivity ($r > 0.6$).

Author Manuscript

Author Manuscript

Author Manuscript

Author Manuscript

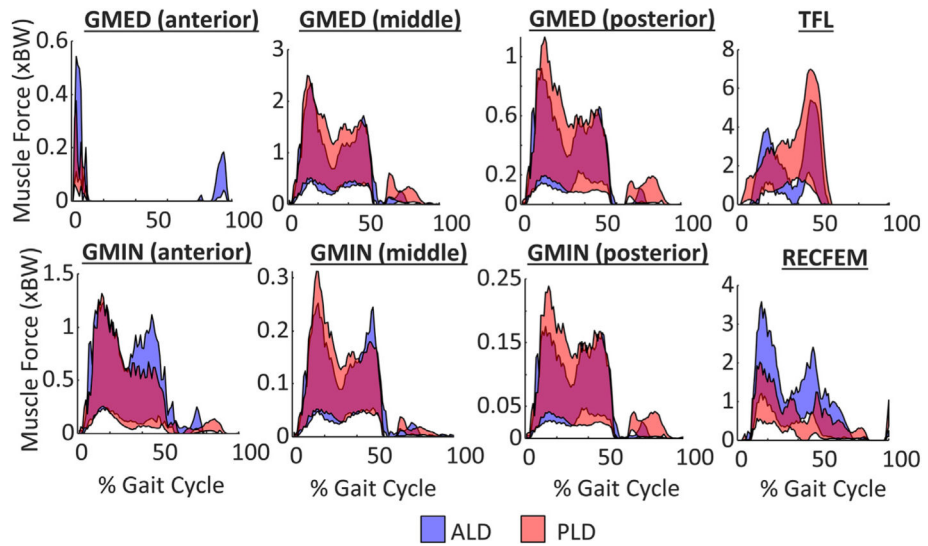


Fig. 6. 99% confidence bounds of hip muscle forces throughout the gait cycle for the anterolateral deficient (ALD – blue) and posterolateral deficient (PLD – red) deficient patients. Note: a positive sensitivity factor indicates a reduction in hip JRF.

Table 1Patient demographics for two representative acetabular dysplasia (AD) subgroup patients (mean \pm SD).

	ALD	PLD
Age (years)	17	31
BMI (kg/m ²)	22.7	21.7
Sex	Female	Female
Symptomatic Hip	Right	Right
Self-Selected Walking Speed (m/s)	1.40	1.46
Lateral center edge angle (deg) (AP view)	18.2	-2.8
Tonnis angle (deg) (AP view)	17	15

Author Manuscript

Author Manuscript

Author Manuscript

Author Manuscript

Table 2

Sensitivity factor between each DOF in the simulated PAO and the abduction and flexion moment arms of the rectus femoris and primary hip abductors of ALD (anterolateral deficient) and PLD (posterolateral deficient). + indicates strong sensitivity ($r > 0.6$) and * indicates moderate sensitivity ($0.4 < r < 0.6$).

Muscle	Moment Arm	Acetabular Adduction						Acetabular Extension						Hip Joint Center Medialization					
		JRF1	ALD	PLD	JRF2	ALD	PLD	JRF1	ALD	PLD	JRF2	ALD	PLD	JRF1	ALD	PLD	JRF2	ALD	PLD
RFEM	Abd	-0.91 ⁺	-0.89 ⁺	-1.00 ⁺	-0.98 ⁺	0.41 [*]	0.45 [*]	0.06	0.20	0.08	-0.02	0.07	-0.02	0.07	-0.02	-0.02	-0.02	0.07	-0.02
	Flex	-0.36	-0.21	-0.01	-0.02	-0.29	-0.21	-0.98 ⁺	0.02	-0.95 ⁺	0.02	-0.04	-0.04	-0.04	-0.04	-0.04	-0.01	-0.04	-0.01
GMED (ant)	Abd	-0.07	0.03	-0.07	0.03	0.05	-0.01	-0.07	0.03	1.00 ⁺	0.99 ⁺	0.99 ⁺	0.99 ⁺	0.99 ⁺	0.99 ⁺	0.96 ⁺	0.96 ⁺	0.96 ⁺	0.96 ⁺
	Flex	-0.07	0.03	-0.07	0.03	0.04	0.00	0.04	0.00	1.00 ⁺	0.88 ⁺	1.00 ⁺	0.96 ⁺	1.00 ⁺	0.96 ⁺	0.96 ⁺	0.96 ⁺	0.96 ⁺	0.96 ⁺
GMED (mid)	Abd	-0.07	0.03	-0.07	0.03	0.04	0.01	0.03	-0.01	0.99 ⁺	1.00 ⁺	0.94 ⁺	1.00 ⁺	0.94 ⁺	1.00 ⁺	1.00 ⁺	1.00 ⁺	1.00 ⁺	1.00 ⁺
	Flex	-0.07	0.03	-0.07	0.03	0.04	-0.01	0.04	-0.01	0.98 ⁺	0.99 ⁺	0.98 ⁺	1.00 ⁺	0.98 ⁺	1.00 ⁺	1.00 ⁺	1.00 ⁺	1.00 ⁺	1.00 ⁺
GMED (post)	Abd	-0.07	0.02	-0.07	0.02	0.05	-0.01	0.05	-0.01	1.00 ⁺	1.00 ⁺	1.00 ⁺	1.00 ⁺	1.00 ⁺	1.00 ⁺	1.00 ⁺	1.00 ⁺	1.00 ⁺	1.00 ⁺
	Flex	-0.07	0.02	-0.07	0.02	0.05	-0.01	0.05	-0.01	1.00 ⁺	1.00 ⁺	1.00 ⁺	1.00 ⁺	1.00 ⁺	1.00 ⁺	1.00 ⁺	1.00 ⁺	1.00 ⁺	1.00 ⁺
GMIN (ant)	Abd	-0.07	0.03	-0.07	0.03	0.05	-0.00	0.04	-0.00	0.99 ⁺	0.98 ⁺	0.99 ⁺	0.96 ⁺	0.99 ⁺	0.96 ⁺	0.96 ⁺	0.96 ⁺	0.96 ⁺	0.96 ⁺
	Flex	-0.07	0.03	-0.07	0.03	0.04	-0.00	0.05	-0.00	0.99 ⁺	0.97 ⁺	1.00 ⁺	0.98 ⁺	1.00 ⁺	0.98 ⁺	0.98 ⁺	0.98 ⁺	0.98 ⁺	0.98 ⁺
GMIN (mid)	Abd	-0.07	0.03	-0.07	0.03	0.04	-0.01	0.04	-0.01	1.00 ⁺	0.99 ⁺	0.99 ⁺	0.99 ⁺	0.99 ⁺	0.99 ⁺	0.99 ⁺	0.99 ⁺	0.99 ⁺	0.99 ⁺
	Flex	-0.07	0.02	-0.07	0.02	0.04	-0.01	0.05	-0.01	0.99 ⁺	0.99 ⁺	1.00 ⁺	0.99 ⁺	1.00 ⁺	0.99 ⁺	0.99 ⁺	0.99 ⁺	0.99 ⁺	0.99 ⁺
GMIN (post)	Abd	-0.07	0.02	-0.06	0.02	0.05	-0.01	0.05	-0.01	1.00 ⁺	1.00 ⁺	1.00 ⁺	1.00 ⁺	1.00 ⁺	1.00 ⁺	1.00 ⁺	1.00 ⁺	1.00 ⁺	1.00 ⁺
	Flex	-0.06	0.02	-0.06	0.02	0.05	-0.01	0.05	-0.01	1.00 ⁺	1.00 ⁺	1.00 ⁺	1.00 ⁺	1.00 ⁺	1.00 ⁺	1.00 ⁺	1.00 ⁺	1.00 ⁺	1.00 ⁺
TFL	Abd	-0.06	0.02	-0.06	0.02	0.05	-0.01	0.05	-0.01	1.00 ⁺	1.00 ⁺	1.00 ⁺	1.00 ⁺	1.00 ⁺	1.00 ⁺	1.00 ⁺	1.00 ⁺	1.00 ⁺	1.00 ⁺
	Flex	0.07	-0.03	0.07	-0.03	-0.04	0.00	-0.05	0.01	-0.99 ⁺	-0.99 ⁺	-1.00 ⁺	-0.99 ⁺	-1.00 ⁺	-0.99 ⁺	-0.99 ⁺	-0.99 ⁺	-1.00 ⁺	-0.99 ⁺